

CO₂-triggered fine tune of electrical conductivity via tug-of-war between ions

| | |
|-------|---|
| メタデータ | 言語: eng 出版者: 公開日: 2019-11-15 キーワード (Ja): キーワード (En): 作成者: メールアドレス: 所属: |
| URL | https://doi.org/10.24517/00056099 |

This work is licensed under a Creative Commons Attribution-NonCommercial-ShareAlike 3.0 International License.





Journal Name

Letter

CO₂-triggered fine tune of electrical conductivity via tug-of-war between ions

Kosuke Kuroda*, Yumiko Shimada and Kenji Takahashi

Received 00th January 20xx,
Accepted 00th January 20xx

DOI: 10.1039/x0xx00000x

www.rsc.org/

A novel approach to control electrical conductivity with CO₂ was proposed by reversible shift of molecular structures between free ions and zwitterions. It was achieved by new design of ionic liquids, possessing dynamic covalent bond between anion and cation. The conductivity was finely tuned by changing partial pressure of CO₂.

Reversible tuning of electrical conductivity of materials is of interest for various applications such as switches, sensors, condensers, and variable resistors. Although there are a number of reports about thermal tuning of electrical conductivity¹⁻³, temperature limitation for use is often a critical issue. Chemical tuning is thus preferable; specifically, dissolving and expelling CO₂ is more preferable owing to its repeatability, safety, and eco-friendly character compared with chemical reagents. Until now, there have been no reports on tuning by CO₂ with transition-type solid conductors. With regard to a solution, tuning by CO₂ bubbling itself can be achieved by shifting molecular structures between neutral and ionic species. However, the usable structures are strictly limited—amidines, amines, and few amine related compounds—and thus the range of application is limited.^{4,5}

Here we propose a totally different way to control the ion mobility by limitation of ion mobility in an electric field, not by shifting the structure between neutral and ionic species. We focused on ionic liquids (ILs), which are basically composed by organic ions (or non-metal inorganic ions).⁶⁻⁹ They are known as good conductive liquids with and without other solvents.¹⁰⁻¹² Unlike metal ions, a wide variety of organic ions exist and the most significant property of organic ions is “having covalent bonds”. By exploiting covalent bonds, we can freely design ions we want by means of various interactions, such as hydrophobic interaction and hydrogen bonds in addition to the covalent

bond itself. Zwitterions (ZIs)¹³⁻¹⁶—anion and cation tethered by a covalent bond—are a unique design of organic ions. They do not move in an electric field^{13,17} because the anion and cation parts tend to move to opposite sides with the same force, like tug-of-war between them. Therefore if the ion structure can be switched between the separated anion and cation and the ZI, a significant shift in conductivity can be achieved.

In this study, we exploited novel organic ions which can switch between the separated ions and the ZI by introducing dynamic covalent bonds to anions and cations. A dynamic covalent bond¹⁸ is a covalent bond that can be formed and broken reversibly by external stimuli, and there are a few reports regarding dynamic covalent bonds between cations of ILs and neutral compounds (not between cation and anion).^{19,20} Especially imine bonds^{21,22} can be formed and broken by pH change. As the pH range of forming/breaking the imine bond depends on the structure of amine and aldehyde²¹, we wonder that IL analogues with suitably designed anions and cations can reversibly shift to ZI even by a small pH change—only adding/expelling CO₂. In this study, we tuned the conductivity of solutions by using the ions tethered by imine bonds. Moreover, if fine-tuning of the conductivity is additionally achieved, variable resistors will be downsized to millimeter- or micrometer-scale because present variable resistors change the resistance by physically shifting the length of the resistance systems and are thus large. While CO₂-driven fine-tuning has not been reported with any compounds, to the best of our knowledge, we realised fine-tuning by changing the partial pressure of CO₂; we expected that the pH of the solution and consequent equilibrium of forming/breaking the imine bond could be controlled based on Henry's law.

We synthesised a novel IL analogue with an imine bond—1-(3-aminopropyl)-3-methylimidazolium benzaldehyde-2-carboxylate ([C_{3NH2}mim][*o*-aldBzCOO], shown in Fig. 1). The structural shift of [C_{3NH2}mim][*o*-aldBzCOO] between the IL form and the ZI form (left- and right hand sides of Fig. 1) in the aqueous solutions was identified by ¹H NMR (Fig. 2 and the full spectra are shown in Fig. S1.). Signals arising from the

Division of Natural System, Graduate School of Natural Science and Technology, Kanazawa University, Kakuma-machi, Kanazawa 920-1192, Japan. Email: kkuroda@staff.kanazawa-u.ac.jp

† Footnotes relating to the title and/or authors should appear here.

Electronic Supplementary Information (ESI) available: experimental details and supporting figures. See DOI: 10.1039/x0xx00000x

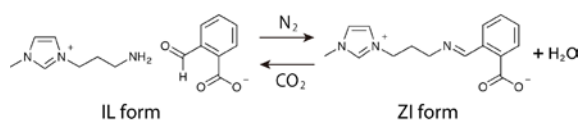


Fig. 1 Structures of the IL- and ZI forms of $[C_{3NH_2}mim][o\text{-aldBzCOO}]$.

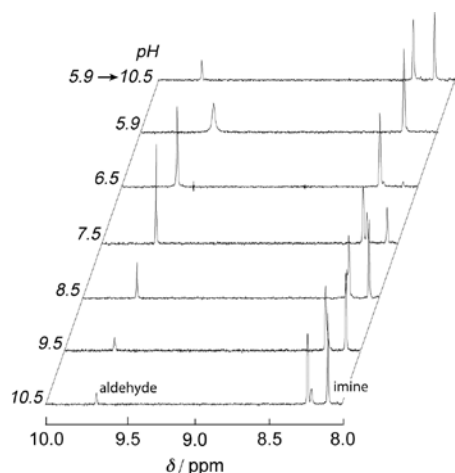


Fig. 2 1H NMR spectra of $[C_{3NH_2}mim][o\text{-aldBzCOO}]$ solutions at pH 10.5, 9.5, 8.5, 7.5, 6.5 and 5.9 and a solution at pH 10.5 reversed from pH 5.9. The solution at pH 9.5 is the original solution. The signals at 8.1 and 9.7 ppm are attributed to the imine (ZI form) and the aldehyde (IL form), respectively.

aldehyde (IL form) and imine (ZI form) were respectively observed at 9.6 and 8.1 ppm. We assessed the structural shift of $[C_{3NH_2}mim][o\text{-aldBzCOO}]$ when changing pH by acid/base to understand the characteristics. The pH of the solution before the addition of acid/base was 9.5, and a relatively large peak at 8.1 ppm and a small peak at 9.6 ppm were observed. This indicates that the majority of $[C_{3NH_2}mim][o\text{-aldBzCOO}]$ exists as ZI form in the solution. When acetic acid was added to decrease the pH, the signal at 8.1 ppm gradually decreased and the signal at 9.6 ppm increased; the ratio of the ZI form decreased and that of the IL form increased. At around pH 6, the signal at 8.1 ppm was completely diminished, indicating complete conversion to the IL form. There was no change below pH 5.9. On the other hand, when NaOH was added to the original solution, both signals were almost unchanged up to pH 12, indicating that the major part of $[C_{3NH_2}mim][o\text{-aldBzCOO}]$ exists as the ZI form under basic conditions.

The ratio of the IL form and the ZI form was calculated from the areas of the signals. The pH dependence of the ratio of the IL form is plotted in Fig. 3. Before the addition of acid/base (pH 9.5), the ratio of the IL form was 16% (the ZI form was 84%). As the pH decreased, the ratio of the IL form drastically increased, reaching 50% at around pH 8. The ratio of the IL form became 100% at around pH 6 and did not change below pH 6. When the pH of the solution increased, the ratio of the IL form was almost the same as in the original solution. From these results, the maximum ratio of the IL form was found to be 100%, and the minimum ratio was found to be around 15%; the ratio drastically varied in solutions between pH 6 and 9.5. In addition, the change of the ratio was reversible. Acetic acid was added to the $[C_{3NH_2}mim][o\text{-aldBzCOO}]$ solution to adjust the pH to 5.9,

followed by addition of NaOH to re-adjust to pH 10.5. The intensity of the signals at 8.1 and 9.6 ppm respectively increased and decreased compared with those at pH 5.9. The ratio of the IL form returned from 100% to 20%, similar to those of the solution at pH 10.5 directly made from the original solution.

We shifted the structure by bubbling the $[C_{3NH_2}mim][o\text{-aldBzCOO}]$ solution with CO_2 and N_2 for decreasing and returning pH. When $[C_{3NH_2}mim][o\text{-aldBzCOO}]$ was bubbled with N_2 , there was no obvious change in the 1H NMR spectrum of $[C_{3NH_2}mim][o\text{-aldBzCOO}]$, as shown in Fig. 4 (the full spectra are shown in Fig. S2); the ratio of the IL form after N_2 bubbling was 14% at pH 9.6 while that of the original solution was 16% at pH 9.5. The slight change may be a result of the expulsion of the dissolved CO_2 that was absorbed from the air. On the other hand, the pH of the solution decreased to 6.3 upon bubbling with CO_2 , and the 1H signals at 8.1 and 9.6 ppm greatly decreased and increased, respectively; the ratio of the IL form increased to 92%. In addition, the structural shift was confirmed to be reversible. A $[C_{3NH_2}mim][o\text{-aldBzCOO}]$ solution was bubbled with CO_2 and then with N_2 . The intensity of the signals at 8.1 and 9.6 ppm significantly increased and decreased, respectively, after N_2 bubbling. The ratio of the IL form returned from 92% to 21%. N_2 bubbling expelled CO_2 , resulting in recovery of the ratio of the IL form. These results indicate that we achieved a structural shift caused even by gas

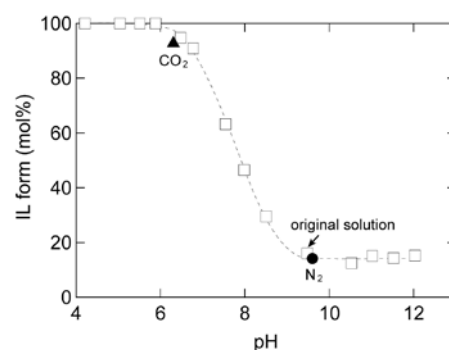


Fig. 3 Relation between pH and ratio of the IL form in the $[C_{3NH_2}mim][o\text{-aldBzCOO}]$ solutions after adding acid/base (open square) and after bubbling with N_2 (closed circle) and CO_2 (closed triangle).

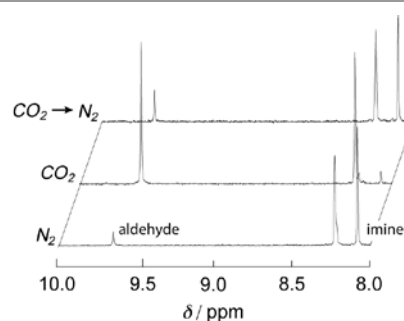


Fig. 4 1H NMR spectra of $[C_{3NH_2}mim][o\text{-aldBzCOO}]$ aqueous solutions after bubbling with N_2 and CO_2 , and a solution bubbled with CO_2 followed by N_2 .

bubbling, which is an efficient alternative to adding acid/base.

To confirm that the structural shift of $[C_{3NH_2}mim][o\text{-aldBzCOO}]$ caused by gas bubbling arises from the pH change, we also plotted the relation between the pH and the ratio of the

IL form after bubbling with N_2 and CO_2 in Fig. 3. As the plots arising from gas bubbling corresponded to the plots of the pH dependence obtained by adding acid/base, it was confirmed that the structural change caused by gas bubbling is the result of a pH change. Although some amines and ILs have ability to capture CO_2 via covalent bond, the cation did not react with CO_2 in this case (details in ESI, Fig. S3). In addition, the pH of the bubbled samples ranged from 6.3 to 9.6, which were almost the end points of the pH range affecting the structure of $[C_{3NH_2}mim][o\text{-aldBzCOO}]$: $[C_{3NH_2}mim][o\text{-aldBzCOO}]$ is the well-designed structure for the shift with CO_2 and N_2 .

The electrical conductivity of the $[C_{3NH_2}mim][o\text{-aldBzCOO}]$ solution was measured (Fig. 5). The conductivity was 0.6 mS/cm before gas bubbling. It increased to 4.3 mS/cm after CO_2 bubbling within 14 min. We thus were able to demonstrate control of the conductivity of the solution in the order of mS/cm, which is comparable to the cases with highly concentrated solutions of optimised amines while almost cases are in the order of $\mu\text{S/cm}$.^{23,24} The results also show that the resistivity of 1700 and 230 Ωcm before and after CO_2 bubbling and the both solutions are recognised as semiconductors; the value of 230 Ωcm is especially similar to silicon at room temperature.²⁵ In addition, it returned to 0.8 mS/cm by N_2 bubbling after 29 h. The return was very slow because expelling CO_2 by N_2 is not very effective. However, it is noted that the half-life period under N_2 bubbling was 2.2 hours and thus not so slow. Furthermore, sonication was confirmed to be one of facilitation methods: the half-life period was 30 min under sonication. The procedure is confirmed to be repeatable at least three times as shown in Fig. 5.

Fine-tuning of the conductivity of the solution with CO_2 was attempted by controlling the ratio of IL form and ZI form, based on partial pressure of CO_2 . Fig. 6 shows the relation between the conductivity and the partial pressure of CO_2 . Only slight partial pressure affected the conductivity; 2.5, 3.4, and 3.8 mS/cm at 1, 5, and 10 kPa (original solution: 0.6 mS/cm). It was finally 4.3 mS/cm at 101 kPa (atmospheric pressure) as we mentioned before. To clarify that the increase in conductivity is based on the structural shift of $[C_{3NH_2}mim][o\text{-aldBzCOO}]$,

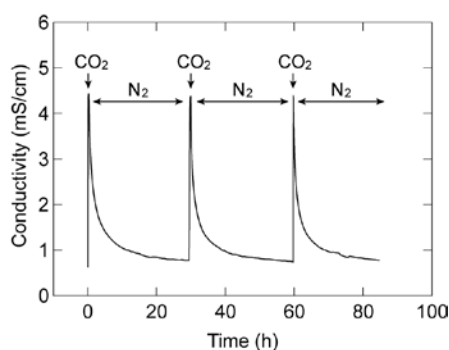


Fig. 5 Conductivity of the $[C_{3NH_2}mim][o\text{-aldBzCOO}]$ solution during bubbling with CO_2 and N_2 .

the relation between the ratio of the IL form and partial pressure of CO_2 was also plotted in Fig. 6. The trend was quite similar to the change of the conductivity; it was drastically

increased in the range of 0–10 kPa (83 mol% at 10 kPa) and gradually increased in the range of 10–101 kPa (93 mol% at 101 kPa). To further confirm that the pH change of the solution was the driving force of the structural shift, the relation between the pH and the ratio of the IL form after CO_2 bubbling at various partial pressures was plotted in Fig. 7. The relation was confirmed to be the same as that changed with acid/base, clearly suggesting that the pH change is the driving force. This is the first report to demonstrate fine tune of conductivity of solutions by CO_2/N_2 bubbling.

Finally, we demonstrated utilisation of the $[C_{3NH_2}mim][o\text{-aldBzCOO}]$ solution as a variable resistor. Fig. 8a shows the electrical circuit used in this study. The circuit is a series circuit and includes an AC power source, an ammeter, a light-emitting diode (LED), and a 1 wt% $[C_{3NH_2}mim][o\text{-aldBzCOO}]$ solution. The solution is depicted as a variable resistor (a photograph of the entire system is shown in Fig. S4). Fig. 8b shows the LED of the system before electrifying in a light room, as a reference. Fig. 8c shows the emission from the LED in a dark room before and after CO_2 bubbling at 0.1, 1, 101 kPa. Only slight emission was observed before CO_2 bubbling. The emission became somewhat stronger after CO_2 bubbling at 0.1 kPa. The intensity of the emission increased with increasing the partial pressure of CO_2 ; it finally became much stronger after bubbling at 101

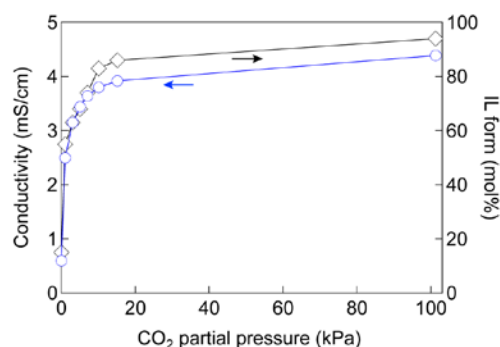


Fig. 6 Conductivity of the $[C_{3NH_2}mim][o\text{-aldBzCOO}]$ solution and the ratio of the IL form after bubbling with CO_2 at different partial pressure.

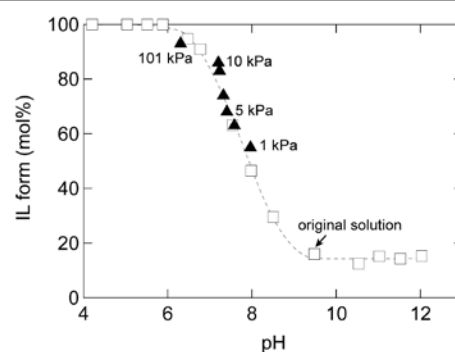


Fig. 7 Relation between pH and ratio of the IL form in the $[C_{3NH_2}mim][o\text{-aldBzCOO}]$ solutions after CO_2 bubbling with various partial pressures (closed triangle). Open squares show the relation between pH and ratio of the IL form in the $[C_{3NH_2}mim][o\text{-aldBzCOO}]$ solutions when controlling pH by acid/base, as references.

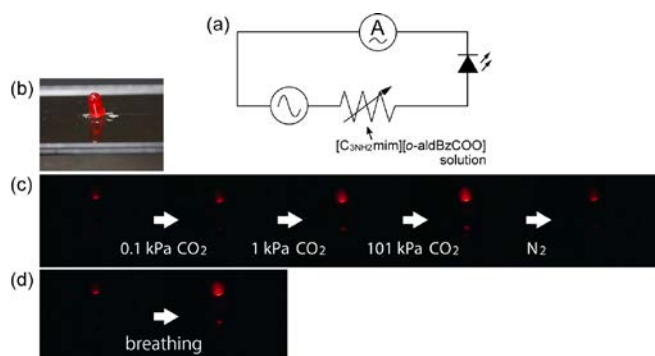


Fig. 8 (a) Circuit diagram of emission experiment. A picture of the actual system is shown in Fig. S2. (b) The light-emitting diode of the system in a light room. (c) Emission from light-emitting diode in a dark room before and after CO₂ bubbling with different partial pressure and N₂ bubbling. Bubbling with 0.1, 1, 101 kPa CO₂ and 101 kPa N₂ was serially conducted. (d) Emission from light-emitting diode in a dark room before and after bubbling with exhaled breath.

kPa. N₂ bubbling moreover achieved return of the emission. The intensity of the emission is basically related to the current value and the trend was also observed in this study: 33 mA before CO₂ bubbling, 44, 50, 68 mA after CO₂ bubbling at 0.1, 1, 101 kPa, and 34 mA after N₂ bubbling. [C₃NH₂mim][o-aldBzCOO] first enabled control of the current by CO₂/N₂ bubbling and consequently worked as a variable resistor. Application of transistors is expected to enable clear on/off and control of much stronger electric currents, while we used only an LED in this study to clarify a potential of [C₃NH₂mim][o-aldBzCOO].

To show further potential of [C₃NH₂mim][o-aldBzCOO], we changed the emission with a device everyone possesses—breathing. Exhaled breath includes 4–5% CO₂ and thus the concentration is enough to cause a change. Fig. 8d shows the emission before and after bubbling with exhaled breath. The emission increased as well as CO₂ bubbling and the current value also increased from 33 to 65 mA. This suggests that electric devices will be operated without any special equipment while the increase of conductivity may be much depending on persons and situations because the composition of the exhaled gases is viable. It is noted that the sophisticated amines for shift of conductivity are generally corrosive and highly toxic, even their vapor, and thus application of the tuning with breathing is not feasible. Therefore, non-volatile ions and zwitterions shown in this study should be suitable. In addition, this novel methodology is expected to be applicable as CO₂ sensor especially in low concentration range.

It is noted here, the electrical conductivity studied in this study includes is the mixed conductivity attributed to both electron and ion conductivities. Each contribution of electron and ion is not clear now and further investigation is one of future works.

In conclusion, we developed a novel methodology to reversibly shift conductivity by CO₂; involving novel design of ILs which reversibly shift to ZIs. The conductivity significantly changed in the order of mS/cm and finely tuned by partial pressure of CO₂. As a result, this is a first report about CO₂-driven variable resistors.

Conflicts of interest

There are no conflicts to declare.

Acknowledgements

This research was supported in part by the COI program of MEXT and JST, and the Advanced Low Carbon Technology Research and Development Program (ALCA) (No. 2100040 to K.T.) of JST. This study was also partly supported by KAKENHI (No. 15K17867 and 18K14281) of JSPS and Leading Initiative for Excellent Young Researchers of MEXT.

Notes and references

- R. G. Moore, J. Zhang, V. B. Nascimento, R. Jin, J. Guo, G. T. Wang, Z. Fang, D. Mandrus and E. W. Plummer, *Science*, 2007, **318**, 615.
- L. A. Bursill and P. J. Lin, *Nature*, 1984, **311**, 550.
- R. Zheng, J. Gao, J. Wang and G. Chen, *Nat. Commun.*, 2011, **2**, 289.
- Y. Liu, P. G. Jessop, M. Cunningham, C. A. Eckert and C. L. Liotta, *Science*, 2006, **313**, 958.
- Z. Guo, Y. Feng, Y. Wang, J. Wang, Y. Wu and Y. Zhang, *Chem. Commun.*, 2011, **47**, 9348.
- R. D. Rogers and K. R. Seddon, *Science*, 2003, **302**, 792–793.
- T. Welton, *Chem. Rev.*, 1999, **99**, 2071.
- M. Armand, F. Endres, D. R. MacFarlane, H. Ohno and B. Scrosati, *Nat. Mater.*, 2009, **8**, 621.
- K. R. Seddon, *Nat. Mater.*, 2003, **2**, 363.
- P. Bonhôte, A.-P. Dias, N. Papageorgiou, K. Kalyanasundaram and M. Grätzel, *Inorg. Chem.*, 1996, **35**, 1168.
- R. Hagiwara and Y. Ito, *J. Fluorine Chem.*, 2000, **105**, 221.
- Q.-G. Zhang, S.-S. Sun, S. Pitula, Q.-S. Liu, U. Welz-Biermann and J.-J. Zhang, *J. Chem. Eng. Data*, 2011, **56**, 4659.
- M. Yoshizawa, M. Hirao, K. Ito-Akita and H. Ohno, *J. Mater. Chem.*, 2001, **11**, 1057.
- K. Kuroda, Y. Kohno and H. Ohno, *Chem. Lett.*, 2017, **46**, 870.
- Y. Ito, Y. Kohno, N. Nakamura and H. Ohno, *Chem. Commun.*, 2012, **48**, 11220.
- K. Kuroda, H. Satria, K. Miyamura, Y. Tsuge, K. Ninomiya and K. Takahashi, *J. Am. Chem. Soc.*, 2017, **139**, 16052.
- H. Satria, K. Kuroda, T. Endo, K. Takada, K. Ninomiya and K. Takahashi, *ACS Sustain. Chem. Eng.*, 2017, **5**, 708.
- S. J. Rowan, S. J. Cantrill, G. R. L. Cousins, J. K. M. Sanders and J. F. Stoddart, *Angew. Chem. Int. Ed.*, 2002, **41**, 898.
- M. D. Soutullo, R. A. O'Brien, K. E. Gaines and J. H. Davis, Jr., *Chem. Commun.*, 2009, 2529.
- M. K. Muthayala and A. Kumar, *ACS Comb. Sci.*, 2012, **14**, 5–9.
- C. Godoy-Alcántar, A. K. Yatsimirsky and J.-M. Lehn, *J. Phys. Org. Chem.*, 2005, **18**, 979.
- N. Giuseppone and J.-M. Lehn, *Chemistry*, 2006, **12**, 1715–1722.
- T. Yu, T. Yamada, G. C. Gaviola and R. G. Weiss, *Chem. Mater.*, 2008, **20**, 5337.
- S. M. Mercer and P. G. Jessop, *ChemSusChem*, 2010, **3**, 467–470.
- H. Sasaki, A. Ikari, K. Terashima and S. Kimura, *Jpn. J. Appl. Phys.*, 1995, **34**, 3426.